# Supporting Information

# Low-Frequency Noise in Bilayer MoS$_2$ Transistor

*Xuejun Xie[1*], Deblina Sarkar[1], Wei Liu[1], Jiahao Kang[1], Ognian Marinov[2], M. Jamal Deen[2], and Kaustav Banerjee[1\*]*
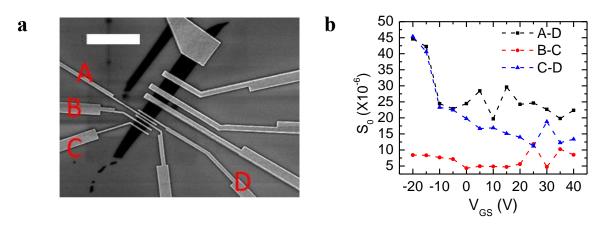
[1]Department of Electrical and Computer Engineering, University of California, Santa Barbara, CA 93106, USA

[2]Electrical and Computer Engineering Department, McMaster University, Hamilton, ON L9H 6J5, Canada

*\*Email: xxie@ece.ucsb.edu; kaustav@ece.ucsb.edu*

## S1. Noise Peak Data in Other Devices

**a**



**b**

**Figure S1.** (a) Device SEM image. The "white" scale bar denotes 5 $\mu m$. (b) $S_0$ measured at room temperature with $V_{DS} = 3\,V$ on electrode A-D, B-C, and C-D with channel length of 130 nm, 376 nm, and 873 nm, respectively.

## S2. Contact Resistance Extraction

In order to extract the contact resistance, two devices with contact electrodes of same dimensions are measured at room temperature with $V_{DS} = 3$ V as shown in Figure S2(a, b). The contact resistance is extracted by calculating the intercept of channel length vs. resistance at different back gate voltages. The extracted contact resistance includes the Schottky junction's resistance. As shown in Figure S2(c), when $V_{GS} < V_T$, the contact resistance increases exponentially, and when $V_{GS} > V_T$, the device resistance is dominated by the channel resistance.
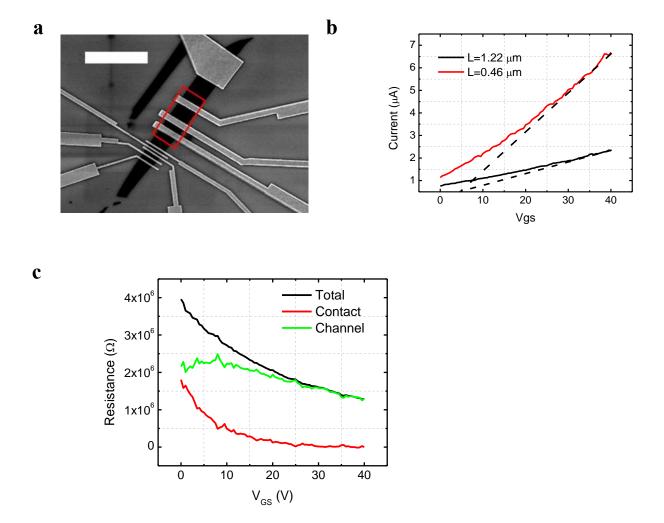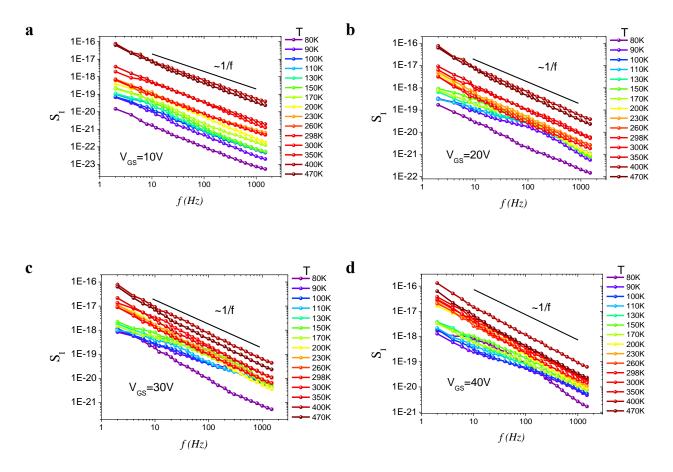
**a**



**b**



**c**



**Figure S2.** (a) The red rectangle marks the two devices measured for contact resistance extraction. The "white" scale bar denotes $5\,\mu m$. The two devices, on the right and on the left, have channel length of

1.22 $\mu m$ and 0.46 $\mu m$, respectively. (b) Drain current at different gate voltage with $V_{DS} = 3$ V. The dashed lines indicate that the threshold voltage $V_T$ is around 5 V. (c) Total resistance, contact resistance and channel resistance (for $L = 1.22\ \mu m$) for different gate voltages at $V_{DS} = 3$ V, at room temperature. Note that $R_{contact}/R_{channel} = 6\%$ when $V_{GS} = 20$ V. With such a small $R_{contact}$, it is valid to assume that the M-shaped noise behavior (Fig. 4) reflects the properties of the MoS$_2$ channel.

## S3. Noise Measurement Setup

The sample was placed in cryostat (Janis Research Corp.) with a turbomolecular vacuum pump (~10 nbar or lower), double-shielded (triaxial) DC ports and isolated chuck. It had variable temperature capabilities from 77 K (liquid nitrogen) to 450 K (heated chuck). The gate and drain voltage biases were provided from low-noise SMUs (source-measurement units) of the Agilent 4156C precision semiconductor analyzer, and the drain current and noise are measured by SR570 low-noise preamplifier and SR785 dynamic signal analyzer. Correction for noise from biasing was not applied, since for each measurement at every frequency and biasing condition, it was verified that the product $S_{VG} \times (g_m)^2 < S_{ID}/10$, where $S_{VG}$ is the noise power spectral density of the gate voltage biasing DC source, $S_{ID}$ is the power spectral density of the measured drain current, and $g_m = \partial I_D / \partial V_G$ is the transistor's transconductance, calculated from the measured DC transfer curves of the transistor. The above inequality indicates that the current noise induced by the noise from the input gate voltage can be neglected.

## S4. Current Noise Power Spectral Density for Different Gate Voltages and Temperatures



**Figure S3.** Current noise power spectral density for (a) $V_{GS} = 10V$ and $V_{DS} = 3V$ (b) $V_{GS} = 20V$ and $V_{DS} = 3V$ (c) $V_{GS} = 30V$ and $V_{DS} = 3V$ (d) $V_{GS} = 40V$ and $V_{DS} = 3V$.

## S5. Discussion about the Mobility Fluctuation Model

Another commonly-used theoretical noise model is the mobility fluctuation model. The mobility fluctuation model was proposed by Hooge to explain the low frequency noise phenomena in high purity bulk crystals,[1] where the surface-to-volume ratio is small. The Hooge's model describes the low frequency noise expressed as: $S = \frac{\alpha I^2}{Nf}$, where $\alpha$ is Hooge's parameter, $I$ is current, $N$ is carrier

number, $f$ is frequency. For mobility fluctuation model, the Hooge's parameter is usually below $10^{-4}$ for bulk materials and independent of $V_G$.[2] While in our case, as shown in Figure S4, the Hooge's parameter is increasing with $V_G$, and the value is three orders of magnitude larger than $10^{-4}$ at high $V_G$.
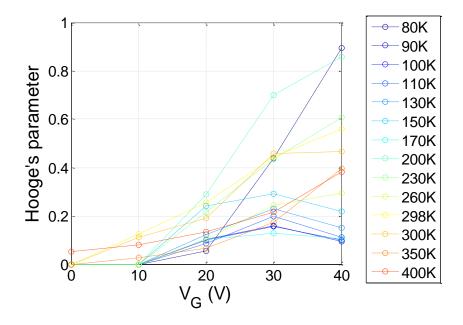


**Figure S4.** Hooge's parameter as function of gate voltage at $V_{DS} = 3$V.

## S6. Density Functional Theory (DFT) Simulation

Since DFT only utilizes periodic boundary conditions, we chose interface unit cells that are periodical in the x and y directions and separated by vacuum in the z direction, as shown in Fig. 5. The unit cell contains a stack of intrinsic MoS$_2$ layer(s) and the surrounding material. For SiO$_2$, we chose a widely adopted crystalline phase (I-42d β-cristobalite), which is similar to amorphous SiO$_2$ in terms of local structure, density and refractive indexes.[3] To model a bulk oxide, the oxide thicknesses are chosen $\geqslant$ 10 Å (6-8 layers) and the dangling O atoms at the bottom are terminated by hydrogen (H) and are fixed at bulk locations to reduce size effects,[4] while all other atoms are allowed to relax.

Numerical DFT calculations are performed using Atomistix ToolKit.[5] Local Density Approximation[6] are used for the exchange correlation potential due to its consistent accuracy for MoS$_2$ interface simulations.[7] A double-$\zeta$ polarized basis set is used for expanding the electronic density. According to the dimensions of the unit cells, *k*-point samplings in the Brillouin zone are 4×8×1. Other parameters are density mesh cut-off = 200 Ry and maximum force =0.05eV/Å for relaxation.

### S7. Discussion about the Numerical Values of $\tau_1$ and $\tau_2$

The values of $\tau_1$ and $\tau_2$ depend on the trap density, carrier density, and electronic potential distribution. By comparing the peak of noise data with the noise model, one can estimate the range of values of the typical time constants for monolayer, bilayer, and trilayer MoS$_2$. Figure S5 shows the $S_0$ contour plot as a function of $\tau_1$ and $\tau_2$ for a wide range of $\tau_2 - \tau_1$, where we can observe that the position of the peak also depends on the range of $\tau_2 - \tau_1$. So, first, we should estimate the value of $\tau_2 - \tau_1$. The range of $\tau_2 - \tau_1$ can be estimated from the $S_I - f$ plot (Fig. 3 in the main article). The $S - f$ plot in Figure S6 shows the noise spectrum with $\tau_1 = 10^{-4}$ s and $\tau_2$ varying from $1\,s$ to $10^{-3}$ s. Comparing with the measured data in Figure 3(a), we observe that all the data are linear in log scale except the data for T=80 K. So we can conclude that the $\tau_2 - \tau_1$ is larger than 0.5 s at room temperature, which is limited by the measured frequency (if we measure the noise at lower frequencies, we may suggest larger $\tau_2 - \tau_1$). The frequency range in previous measurements reported in the literature is 1 Hz to $10^4$ Hz,[8] and 3 Hz to $10^4$ Hz,[9] which can give similar value of $\tau_2 - \tau_1$. Second, we can estimate $\tau_1$. By increasing the carrier density, the noise will encounter a peak as shown by the black dashed line in Figure S5(c), at which condition the $\tau_1$ is about $1.1 \times 10^{-4}$ s. So for monolayer MoS$_2$, the $\tau_1$ is smaller than $1.1 \times 10^{-4}$ s; for bilayer MoS$_2$, the $\tau_1$ is around $1.1 \times$

$10^{-4}$ s; for trilayer MoS$_2$, $\tau_1$ is larger than $1.1 \times 10^{-4}$ s. The $\tau_2$ for those data should be larger than 0.5 s.
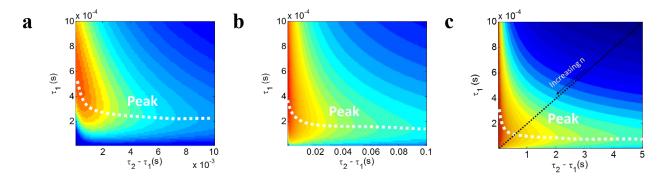


**Figure S5.** The S$_0$ contour map for different ranges of $\tau_2 - \tau_1$. The white dashed lines show the location of noise peak. The black dashed line in (c) shows the change of S$_0$ with the increase in carrier density. The crossing point of white and black dashed lines gives the location of the noise peak, where $\tau_1 = 1.1 \times 10^{-4}$ s.
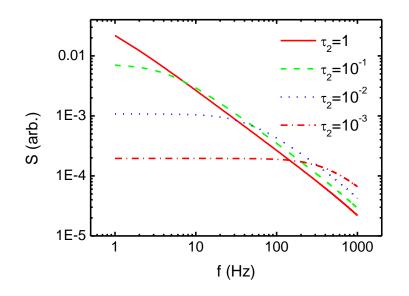


**Figure S6.** The noise spectrum calculated using equation (4) with $\tau_1 = 10^{-4}$ s and $\tau_2$ varying from 1 s to $10^{-3}$ s.

## References:

1.      Hooge, F. N. 1/F Noise Sources. *IEEE Trans. Electron Devices* **1994**, *41*, 1926–1935.

2.      Vandamme, L. K. J.; Rigaud, D. 1/f Noise in MOS Devices, Mobility or Number Fluctuations? *IEEE Trans. Electron Devices* **1994**, *41*, 1936–1945.

3.      Jiang, D.; Carter, E. First-Principles Study of the Interfacial Adhesion between SiO$_2$ and MoS$_2$. *Phys. Rev. B* **2005**, *72*, 165410.

4.      Shan, T.-R.; Devine, B. D.; Phillpot, S. R.; Sinnott, S. B. Molecular Dynamics Study of the Adhesion of Cu/ SiO$_2$ Interfaces Using a Variable-Charge Interatomic Potential. *Phys. Rev. B* **2011**, *83*, 115327.

5.      QuantumWise. Atomistix ToolKit.

6.      Perdew, J. P.; Wang, Y. Accurate and Simple Analytic Representation of the Electron-Gas Correlation Energy. *Phys. Rev. B* **1992**, *45*, 13244–13249.

7.      Kang, J.; Sarkar, D.; Liu, W.; Jena, D.; Banerjee, K. A Computational Study of Metal-Contacts to beyond-Graphene 2D Semiconductor Materials. *IEEE International Electron Devices Meeting*; 2012; pp. 407–410.

8.      Sangwan, V. K.; Arnold, H. N.; Jariwala, D.; Marks, T. J.; Lauhon, L. J.; Hersam, M. C. Low-Frequency Electronic Noise in Single-Layer MoS$_2$ Transistors. *Nano Lett.* **2013**, *13*, 4351–4355.

9.      Wang, Y.; Luo, X.; Zhang, N.; Laskar, M. R.; Ma, L.; Wu, Y.; Rajan, S.; Lu, W. Low Frequency Noise in Chemical Vapor Deposited MoS$_2$. *arXiv* **2013**, *1310.6484*.